Isospin Purity and Delayed-Proton Decay: ^{17}Ne and ^{33}Ar†

J. C. Hardy,* John E. Esterl, R. G. Sextro, and Joseph Cerny
Lawrence Radiation Laboratory and Department of Chemistry, University of California, Berkeley, California 94720
(Received 8 October 1970)

β-delayed proton and γ-ray measurements have been used to study the decay of ^{17}Ne and ^{33}Ar. Their half-lives have been measured as 109.0 ± 1.0 and 173.0 ± 2.0 msec, respectively, and absolute ft values have been determined for their β-decay branches. Precise level energies have been measured in ^{17}F and ^{33}Cl, and an earlier discrepancy concerning energies in ^{17}F has been resolved. The logft value for the superallowed decay branch of ^{17}Ne has been measured to be $3.29^{+0.04}_{-0.07}$, which indicates an isospin purity of $\geq 95\%$ for the lowest $T = \frac{3}{2}$ state in ^{17}F. In addition, the antianalog configuration is located in ^{17}F and is shown to be the most probable source of the small isospin mixing present in the analog state in that nucleus. The logft value measured for the superallowed decay branch from ^{33}Ar was 3.34 ± 0.05, a value which suggests an impurity of ~10% in the lowest $T = \frac{3}{2}$ state in ^{33}Cl. There is circumstantial evidence that this mixing occurs with four $T = \frac{1}{2}$ states which lie within 350 keV of the analog state.

I. INTRODUCTION

The nuclei ^{17}Ne and ^{33}Ar are delayed-proton precursors. They decay by emitting positrons to levels in ^{17}F and ^{33}Cl, respectively, many of which are above the proton separation energy. These decay branches are characterized by the further emission of "delayed protons" with discrete energies corresponding to levels in the final nuclides ^{16}O and ^{32}S. The protons are "delayed" by the preceeding β^+ decay and exhibit its half-life. By precise measurement of the energies and intensities of these proton groups it is possible not only to accurately locate states in the β^+-decay daughter nucleus but also to determine the strength of the β^+ transitions feeding them.

If all the β^+ transitions lead to proton-unstable states, then a simple measurement of the *relative* intensities of the emitted proton groups yields the *absolute* intensity (or ft value) of the corresponding β^+-decay branches. In practice, this is generally not the case. There are usually transitions to states below the proton separation energy whose total intensity must be determined before absolute transition strengths can be deduced. This problem may be overcome by observing γ rays from the deexcitation of proton-stable states and, where this is not possible, by calculating intensities based on the known mirror β^+ transitions. With these methods it is possible to characterize even very weak β^+-decay branches with a precision not usually afforded by other techniques.

Both $^{17}_{10}\mathrm{Ne}_7$ and $^{33}_{18}\mathrm{Ar}_{15}$ have isospin $T = \frac{3}{2}$ ($T_z = -\frac{3}{2}$). One of the decay branches observed from each nuclide feeds its $T = \frac{3}{2}$ analog in the daughter $T_z = -\frac{1}{2}$ nucleus. Such superallowed transitions have very low ft values (logft ~3.3), and to the extent that the initial and final states are truly analogous (i.e., that they have identical wave functions and differ only in T_z), their ft values can be calculated – to a few percent – model independently. Thus, any significant deviation of the measured ft value from the corresponding calculation must arise from differences between the initial and final nuclear wave functions. The $T = \frac{3}{2}$ final state is at relatively high excitation in a $T_z = -\frac{1}{2}$ nucleus and consequently is surrounded by states whose isospin is $T = \frac{1}{2}$. Such states, of course, are not present in the parent nucleus itself, so that any differences that occur between the analog $T = \frac{3}{2}$ states should be due primarily to admixtures of $T = \frac{1}{2}$ configurations in the final state.

Although the $T = \frac{3}{2}$ analog states in the β^+-decay daughter nuclei ^{17}F and ^{33}Cl are unbound to proton emission, only $T = 0$ states in the residual ^{16}O and ^{32}S nuclei are energetically available. This means that proton decay occurs only through isospin impurities in the wave functions involved – presumably, mostly through admixtures in the $T = \frac{3}{2}$ states in ^{17}F and ^{33}Cl. Thus, while the retardation of the β^+-decay feeding the analog state yields quantitatively the amount of its isospin impurity, qualitative information about the actual configuration of the admixed components may be deduced, in principle at least, from the nature of the state's proton decay.

The sensitivity of our method for observing isospin impurities is determined by two factors. The first is the statistical accuracy of the experimental measurements, the second is the reliability of calculations for that small part of the β^+-transition strength which is model dependent: the Gamow-Teller matrix element. For the two superallowed decay branches which will be described here,

these factors are such that an impurity of $\gtrsim 5\%$ could be determined. How does this compare with the anticipated strength of mixing between states with different isospin? Some calculations have been attempted for the mass-9 isobaric quartet, prompted by the existence of rather accurate mass measurements for all four of its lowest-energy members.[1] These measurements indicate that the masses of members of this particular isobaric multiplet, when expressed as a function of T_z, apparently show a small but nonzero dependence upon T_z^3. One plausible explanation of such a cubic dependence is that mixing occurs with $T=\frac{1}{2}$ states present in the $T_z=\pm\frac{1}{2}$ members of the multiplet and, if so, admixtures of up to 17% have been proposed.[2] There are experimental[3] and theoretical[4] reasons for doubting that such a large isospin impurity exists for mass 9, and no similar dependence of the quartet masses on T_z^3 has been observed for mass 13.[5] Nevertheless, estimates[6] of impurities present in the ground and low excited states of nuclei with $16\lesssim A\lesssim 34$ range as high as 2% and it seems entirely possible that mixing in excess of 2% could occur for the $T=\frac{3}{2}$ states which we observe at higher excitation in ^{17}F and ^{33}Cl.

Delayed protons following ^{17}Ne decay[7-11] and ^{33}Ar decay[12-15] have previously been observed. These measurements were restricted by significant background, a limited observable energy range ($E_{\rm lab}\gtrsim 2.5$ MeV) and poor resolution. In the present measurements we have attempted to reduce the background to negligible proportions and at the same time to extend the range of observable energies down to 1 MeV eliminating, it was hoped, the possibility of there being any significant unobserved proton groups. This was accomplished by transferring the delayed-proton precursors by means of a fast gas-transport system to a shielded counting chamber remote from the target position. A cooled counter telescope and particle identification ensured that optimum energy resolution was achieved and that only protons were recorded. γ-ray spectra were recorded simultaneously. In this way reliable absolute ft values have been obtained for many branches including those which are superallowed, and the isospin purity has been determined for the $T=\frac{3}{2}$ states in ^{17}F and ^{33}Cl. For the latter, there is strong evidence that considerable mixing does occur – perhaps totaling 10% – with nearby $T=\frac{1}{2}$ states.

II. THEORY

A. Superallowed β Decay and Isospin Purity

The intensity of any allowed β transition can be expressed in terms of its ft value. The factor f is the "statistical rate function" which takes account of the dependence of transition strength on the total energy release and nuclear charge. The partial half-life t is derived from experiment; it depends upon the measured total half-life and the fraction of all decays which proceed by the particular branch being examined. Expressed in this way, the strength can be directly related to nuclear matrix elements[16,17]

$$ft=\frac{2\pi^3(\ln 2)(\hbar^7/m_0{}^5c^4)}{g_V{}^2\langle 1\rangle^2+g_A{}^2\langle\sigma\rangle^2}\ ,$$

$$=\frac{6.19\times 10^3}{\langle 1\rangle^2+1.41\langle\sigma\rangle^2}\ \text{sec}\ . \tag{1}$$

Here g_V and g_A are the vector and axial-vector coupling constants; the numerical form of the equation results from using the best current values[16] for g_V and g_A/g_V. The symbols $\langle 1\rangle$ and $\langle\sigma\rangle$ stand for the Fermi and Gamow-Teller matrix elements, respectively. The Fermi matrix element for a β^+ transition between an initial state $|\psi_i(J_i,T_i)\rangle$ with spin and isospin (J_i,T_i), and a final state $|\psi_f(J_f,T_f)\rangle$ is given by

$$\langle 1\rangle=\langle\psi_f(J_f,T_f)|\sum_n\tau_+(n)|\psi_i(J_i,T_i)\rangle\ , \tag{2}$$

where τ_+ is the isospin ladder operator which changes a proton into a neutron, and the summation over n extends to all nucleons. Clearly the matrix element is zero unless

$$J_f-J_i=T_f-T_i=0\ . \tag{3}$$

For the decays of ^{17}Ne and ^{33}Ar, $T_i=\frac{3}{2}$; and in the case of the superallowed decay branch, we consider an isospin-mixed final-state wave function $|\chi_f(J_f)\rangle$ written

$$|\chi_f(J_f)\rangle=a|\psi_f^a(J_f,T=\tfrac{3}{2})\rangle+b|\psi_f^b(J_f,T=\tfrac{1}{2})\rangle\ , \tag{4}$$

where $a^2+b^2=1$. Substituting this wave function into Eq. (2) for the Fermi matrix element, one readily obtains

$$\langle 1\rangle^2=[T(T+1)-T_{zi}T_{zf}]a^2=3a^2\ , \tag{5}$$

where we have neglected the effects of mixing with states of $T\geq\frac{3}{2}$. The matrix element has been squared, since that is the form in which it appears in determining the transition strength [Eq. (1)]. The factor a^2 is the fraction of the final-state wave function which has $T=\frac{3}{2}$; that is, it is the isospin purity of the analog state. Similarly, in the case of ordinary allowed decay to states whose predominant isospin is $T=\frac{1}{2}$, a^2 becomes a measure of the $T=\frac{3}{2}$ isospin admixture arising from mixing with the analog state. In such cases a^2 can be related by second-order perturbation theory to the off-diagonal matrix element of the charge-depen-

dent part H_c of the total Hamiltonian:

$$\langle T=\tfrac{3}{2}, T_z=-\tfrac{1}{2}|H_c|\tfrac{1}{2}, -\tfrac{1}{2}\rangle = (E_{3/2}-E_{1/2})\times a \ . \qquad (6)$$

Here E_T corresponds to the energy of the state whose predominant isospin is T, and H_c contains all charge-dependent terms including the Coulomb interaction. It should be emphasized that we have assumed that the $T=\frac{3}{2}$ wave function is the same for all members of a multiplet; this will be true provided the non-Coulomb charge dependence in the nuclear force is also small.

In the preceding discussion of the Fermi matrix element it has been unnecessary to specify any details of the wave functions except their total spin and isospin. The Gamow-Teller matrix element depends upon the evaluation of $\langle\psi_f|\sum_n \sigma(n)\tau_+(n)|\psi_i\rangle$ and necessitates a specific model to describe the wave functions. Its selection rules require

$$\begin{aligned} &|J_f - J_i| = 0, 1 \quad 0 \not\to 0 \ , \\ &|T_f - T_i| = 0, 1 \ . \end{aligned} \qquad (7)$$

Thus, it contributes additional strength to the superallowed decay branches from ^{17}Ne and ^{33}Ar, and a reasonable estimate for its magnitude must be made before the value of a^2, the isospin purity, can be extracted from the experimental decay rate. Calculations have been made[17] for $\langle\sigma\rangle^2$ using the Nilsson model where the relevant nuclear deformations were determined from measured magnetic moments. Comparison with 11 experimental $T=\frac{1}{2}$ mirror transitions[17] in the range $17 \leq A \leq 39$ indicated surprisingly good agreement between the predicted matrix elements $\langle\sigma\rangle^2$ and those values extracted from the experimental data; in all but two cases they disagree by less than 10%. The same methods applied to the decay of ^{17}Ne and ^{33}Ar yielded the following results[17]:

$$\begin{aligned} \langle\sigma\rangle^2 &= 0.11 \ , \quad {}^{17}\mathrm{Ne} \ , \\ &= 0.28 \ , \quad {}^{33}\mathrm{Ar} \ . \end{aligned} \qquad (8)$$

By referring to Eqs. (1) and (5) it can be seen that $\langle\sigma\rangle^2$ will contribute only about 5% for ^{17}Ne and 12% for ^{33}Ar to the total superallowed transition strength (assuming $a^2 \sim 1$). Thus, even relatively large uncertainties in these model calculations will only affect the calculated transition strength by a few percent.

Finally, it is important to realize that if $a^2 = 1$, then for decay between $T=\frac{3}{2}$ states

$$ft \leq 2.06\times 10^3 \text{ sec} \qquad (9)$$

and consequently any experimental violation of this limit can *only* be interpreted as arising from the presence of isospin impurities.

B. Allowed β Decay and Mirror Symmetry

The nucleus ^{33}Ar can undergo an allowed decay to the ground state of ^{33}Cl. Since this decay branch is not followed by particle or γ emission we must deduce its intensity from the known mirror decay,[18] viz., $^{33}\mathrm{P} \xrightarrow{\beta^-} {}^{33}\mathrm{S}$, so that absolute intensities may be deduced for the other observed branches. The intensity of an ordinary allowed transition is given by Eq. (1) where, of course, $\langle 1\rangle^2 = 0$. Assuming mirror symmetry, the decay $^{33}\mathrm{Ar} \xrightarrow{\beta^+} {}^{33}\mathrm{Cl(g.s.)}$ should have the same ft value as the ^{33}P ground-state decay. However, Wilkinson[19] has recently pointed out that known discrepancies between mirror transition rates are consistent with the existence of second-class currents and, in particular, with an induced tensor coupling.[20] An analysis of existing data[19] combined with more recent results[21] indicates the expected proportionality

$$\delta = [(ft)^+/(ft)^-] - 1 \propto (W_0^+ + W_0^-) \ , \qquad (10)$$

where the superscripts + and − refer to positron and electron decay, respectively, and W_0 is the total decay energy. The constant of proportionality is $\sim 5.2\times 10^{-3}$ MeV^{-1} which, for the case of ground-state transitions in mass 33, indicates that $(ft)^+$ exceeds $(ft)^-$ by ~6%. This value was used in the analysis of the ^{33}Ar data, but to take account of the many uncertainties in the procedure a large error was adopted, i.e., $\delta = +0.06 \pm 0.10$.

C. First-Forbidden β Decay

The nucleus ^{17}Ne ($J^\pi = \frac{1}{2}^-$) exhibits weak transitions to the ground state ($\frac{5}{2}^+$) and first excited state ($\frac{1}{2}^+$) of ^{17}F. Both transitions are first forbidden, the ground-state branch being unique first forbidden. Their weakness (~2% of the total decay strength) and the fact that the final states are proton stable prohibits our observing them experimentally, so again predictions must be made based on the known mirror decay[22] of ^{17}N. It is not, however, correct to assume identical ft values for such transitions, since in general the energy spectrum of β particles in forbidden decay differs from that for allowed decay.

The generalized statistical rate function is written[23]

$$f_n = \int_1^{W_0} p_e W_e (W_0 - W_e)^2 F(Z, W_e) C_n dW_e \ , \qquad (11)$$

where n is the order of forbiddenness, $F(Z, W_e)$ is the Fermi function, and C_n is the relevant shape factor. For allowed decay C_0 is a constant, but in first-forbidden decay

$$C_1(W_e) \propto 1 + aW_e + b/W_e + cW_e^2 \ , \qquad (12)$$

where the coefficients a, b, and c are complicated

functions of six nuclear matrix elements which combine coherently, and some of which change sign in going from β^+ to β^- decay. A considerable simplification results for unique first-forbidden decay (i.e., where $|J_f - J_i| = 2$), since five of the six matrix elements vanish. In that case $b = 0$ and the ratio f_1/f_0 has been calculated as a function of Z and W_0,[24] the only remaining matrix element having factored out. The situation is the same as for allowed decay except that $f_1 t$ rather than $f_0 t$ (or ft) is assumed identical for both β^+ and β^- decay. This applies to the ground-state decay branches ($\frac{1}{2}^- \rightarrow \frac{5}{2}^+$) in the mass 17 nuclei.

The decay branches leading to the first excited states of ^{17}F and ^{17}O ($\frac{1}{2}^- \rightarrow \frac{1}{2}^+$) involve five out of the six possible matrix elements, and without model calculations for each the exact relationship of the mirror decays to one another is uncertain. In our analysis of the ^{17}Ne decay we have adopted an ft value for this branch which is midway between the values determined by the procedures relevant to allowed decays and to unique first-forbidden ones. Error bars were assigned, however, to overlap both limits. Only in the unlikely event of strong coherence between matrix elements as they influence the shape factor [Eq. (12)] will these limits be exceeded.

III. EXPERIMENTAL PROCEDURE

The delayed-proton precursors ^{17}Ne and ^{33}Ar were produced by the reactions ^{16}O(^{3}He, $2n$)^{17}Ne and ^{32}S(^{3}He, $2n$)^{33}Ar initiated with external ^{3}He beams from the Berkeley 88-in. cyclotron. In order to examine their decay in an environment as free as possible from extraneous activity, a system was devised which permitted fast transport of the neon and argon isotopes from the position of bombardment to a shielded counting chamber. A detailed explanation of the equipment will be published separately,[25] so only a brief description will be given here.

The experimental arrangement used for the production of ^{33}Ar is shown in Fig. 1. To produce maximum activity, it was necessary to run with as high a beam current as possible on a target which would not deteriorate during prolonged high-current bombardment. No solid target satisfied these conditions, so CS_2 vapor was used. At room temperature CS_2 has a vapor pressure of about $\frac{1}{2}$ atm. Noting Fig. 1, when solenoid valve 1′ between the CS_2 flask and the 20-cc target chamber operates, vapor fills the evacuated chamber which has 2.5-μ Havar foils at each end. At the same time valve 1 opens and closes, filling a ballast chamber with about 1.5 atm of helium. After a predetermined bombarding time, valves 2 and 2′ open and the vapor, together with the recoil atoms produced during bombardment, is swept by the helium gas towards a dry-ice trap. Here the CS_2 is condensed and the liquid collects above valve 3. The helium gas and argon continue past valve 4, which has opened, and into the counting chamber. When valve 4 closes, the counting cycle begins. At this point valves 1 and 1′ reopen and a fresh bombardment begins. Valves 3 and 3′ are also opened to allow the trapped liquid CS_2 to drip into the liquid-nitrogen trap and to allow the line between valves 2′ and 4 to be pumped out in preparation for the next sequence. After the counting cycle is complete, valve 5 is opened and the contents of the counting chamber are pumped away. This entire sequence is repeated every second, so the CS_2 flask must be heated in order to maintain a tem-

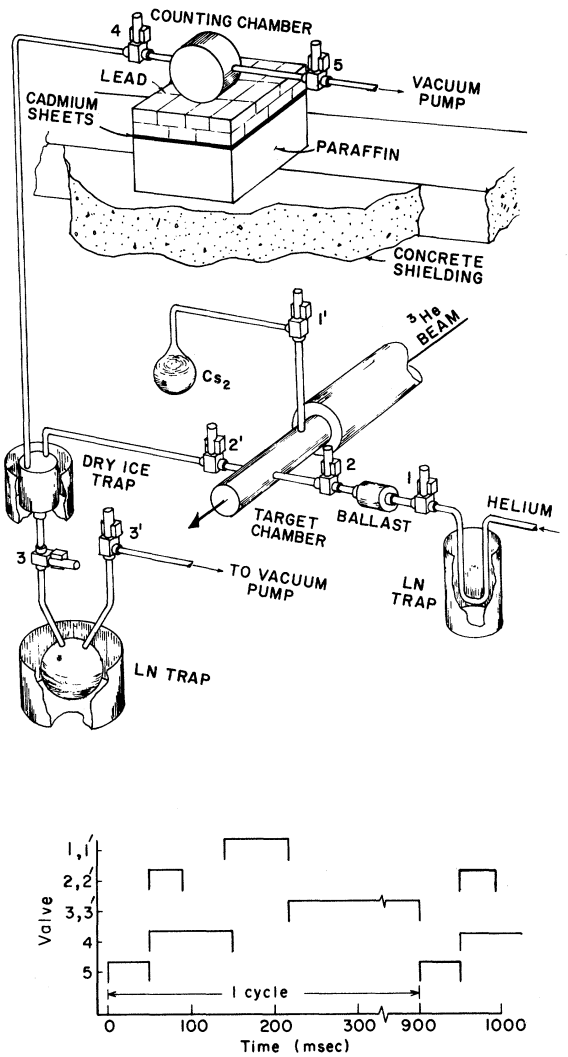

FIG. 1. A schematic diagram of the apparatus used for the production of ^{33}Ar from the reaction ^{32}S(^{3}He, $2n$)^{33}Ar. The sequence of valve operation is shown at the bottom; valve *open* times are indicated.

perature of about 25°C. A typical timing sequence is shown at the bottom of the figure.

Two different techniques employing essentially the same equipment were used in the production of ^{17}Ne. The first technique involved oxygen gas as the target; the CS_2 flask in Fig. 1 was replaced by a cylinder of compressed oxygen, and the dry-ice trap was removed, although access to the vacuum pump through valves 3 and 3′ remained. The second technique used TiO_2 solid targets. Six oxidized titanium foils were stacked 0.5 mm apart in a modified target chamber; helium gas periodically swept through valves 2 and 2′, picking up the recoil nuclei and transporting them past two liquid-nitrogen traps on their way to the counting chamber. In this configuration the line from the target chamber to valve 1′ was removed. Generally, when ^{17}Ne was being produced, the length of time valve 3 remained open was reduced from ~700 to ~400 msec; this shortened the cycle time to accomodate the shorter half-life of ^{17}Ne.

A pressure transducer was mounted in the counting chamber in order to measure the instantaneous pressure. The active volume of the counting chamber was conical, with a total capacity of ~65 cc. The transit time necessary for gas to move the 5 m from the target chamber to the counting chamber was ~100 msec, and the pressure in the chamber during the counting period was ~35 Torr.

A counter telescope was mounted in the counting chamber at the apex of the cone. It consisted of a phosphorus-diffused silicon ΔE transmission counter which, depending upon the experiment, ranged in thickness from 14 to 50 μ, and a 1.0-mm lithium-drifted silicon E counter. The signals from both counters were required to be in coincidence ($2\tau \approx 15$ nsec) before being fed to a Goulding-Landis particle identifier[26] which produced an output signal characteristic of the particle type. Only events corresponding to protons (or, when desired, α particles) were recorded. The counters were cooled to −30°C by means of a liquid-nitrogen cold finger. No obstruction was placed between the ΔE counter and the gas in the counting chamber; this permitted optimum resolution to be obtained. The electronic resolution (full width at half maximum) measured with a pulser was 35 keV and proton peak widths of 45 keV were recorded for narrow states. The additional width of the proton peaks was due principally to the fact that even those protons originating from narrow states exhibit an energy spread caused by the momentum of the preceding positron. With a 14-μ ΔE counter, α particles with energies above ~4 MeV could be identified. To search for lower-energy α particles, the energy signal from the ΔE counter, in anticoincidence with the E-counter signal, was recorded separately.

The efficiency of the counter telescope was calculated by two methods. The first was by actual numerical integration over the active volume, and the second was by recording the proportion of detected events generated by a Monte Carlo computer program. The two calculations gave results which differed by less than 10%, and the value adopted for the efficiency was $(1.26 \pm 0.13) \times 10^{-3}$, which corresponds to an effective solid angle of $(1.58 \pm 0.16) \times 10^{-2}$ sr. With such an arrangement, the number of protons recorded was ~1 per μC of integrated beam current. Thus, at a typical beam current of 3 μA, about 2.5×10^5 events were recorded in a 24-h run.

Lifetimes were measured by two methods. First, total-energy signals corresponding to protons were time-sorted into eight groups of a 4096-channel analyzer, thus providing eight-point decay curves for all statistically significant peaks in the spectrum. Second, a single-channel analyzer was set around a prominent peak in the spectrum, and these events were recorded in a 400-channel analyzer operated in its multiscale mode. The channel address was advanced by a quartz-crystal oscillator, the cycle being commenced with the closing of valve 4.

As a check of our systematic accuracy in measuring half-lives, the decay of ^{9}C was observed, since its half-life had previously been determined quite accurately by two groups.[27,28] The activity was produced using the reaction ^{10}B$(p, 2n)^9$C at 43 MeV, the target being boric acid enriched to 92.4% in ^{10}B. The material was pressed (at 2000 lb/in.^{2}) in 100-mesh tungsten screen,[29] and five such screens were stacked in the target chamber in the same manner as were the TiO_2 targets already described. Oxygen gas was used instead of helium to sweep the ^{9}C recoils to the counting chamber. No traps were used.

Both decay studies required γ-ray measurements. To fully examine the decay of ^{17}Ne, it was necessary to investigate proton-γ coincidences. For this purpose, a 2-in. × 2-in. NaI(Tl) crystal was mounted externally at the base of the conical counting volume, and coincident events ($2\tau \approx 50$ nsec) were recorded two-dimensionally using an on-line PDP-5 computer. Similarly, to obtain higher-resolution γ spectra necessary for deciphering the ^{33}Ar decay, a 45-cc Ge(Li) counter was mounted in the same external position. Energy resolution of ~4 keV at 1 MeV was obtained.

The total efficiency of the Ge(Li) counter was measured as a function of γ energy using the known ^{56}Co spectrum[30] to establish the relative dependence upon energy, and the calibrated[31] γ sources ^{203}Hg, ^{22}Na, ^{54}Mn, and ^{60}Co, to fix the absolute

scale. To determine the dependence of the efficiency upon position in the counting chamber, the ^{56}Co source was moved to various measured locations. Simple geometric formulas were used to interpolate between measured points, and the results were integrated over the active volume. The resultant over-all efficiency evaluated, for example, at 800 keV was $(5.6 \pm 0.3) \times 10^{-4}$.

An additional check on the efficiency of the counter telescope and Ge(Li) counter was afforded by a simultaneous measurement of the number of α particles and 388-keV γ rays emitted in the decay of ^{249}Cf. The ratio of α-particles to γ rays determined using the efficiencies already described agreed with the previously measured value[32] to within 2%.

IV. EXPERIMENTAL RESULTS

A. Identification

Spectra of delayed protons observed following 45-MeV ^{3}He bombardment of oxygen targets are shown in Figs. 2 and 3. The 50-μ ΔE counter used to acquire the spectrum in Fig. 2 prevented protons with $\lesssim$2.5 MeV from being identified, since they could not penetrate to the E counter. By using a 14-μ ΔE counter, protons could be observed down to ~1.0 MeV as shown in Fig. 3; however, in this case protons $\gtrsim$8.0 MeV lose too little energy in the ΔE counter to be reliably observed. Figures 4 and 5 show delayed-proton spectra following ^{3}He bombardment of CS_2 targets; the former utilized a 35-MeV ^{3}He beam and the latter, 55 MeV.

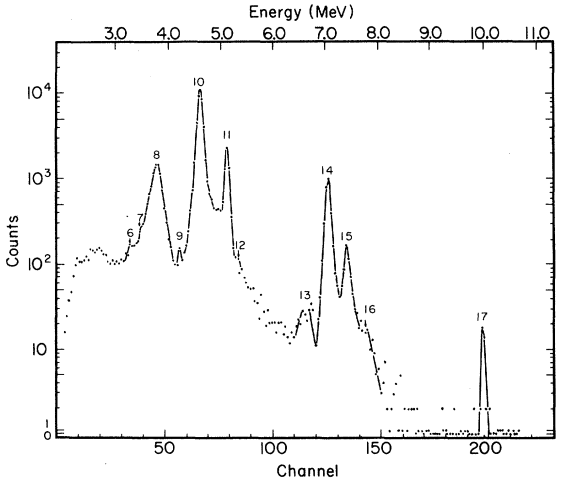

FIG. 2. Spectrum of delayed protons observed in a counter telescope with a 50-μ ΔE counter following 45-MeV ^{3}He bombardment of TiO_2. The proton laboratory energy is indicated at the top. All peaks are identified with the decay of ^{17}Ne, and are numbered to correspond with the data in Table I.

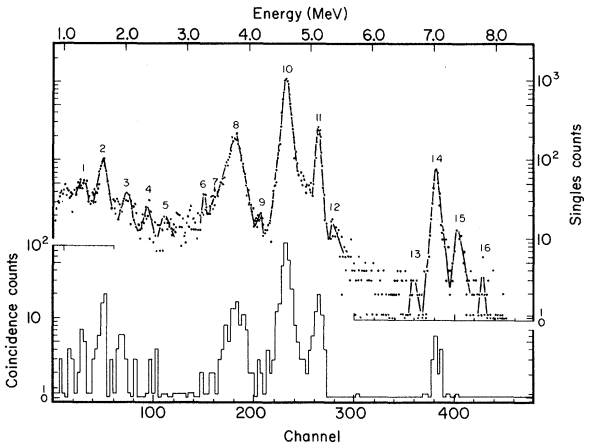

FIG. 3. Spectrum of delayed protons observed in a counter telescope with a 14-μ ΔE counter. The conditions are the same as in Fig. 2. The histogram at the bottom of this figure represents those events which were observed in coincidence with 511-keV γ rays. (When two-channel averages are taken, no peaks appear between those numbered 5 and 6.)

The calculated threshold for production of ^{17}Ne by the reaction ^{16}O(^{3}He, $2n$)^{17}Ne is 26.68 MeV.[1] Only two other delayed-proton precursors can be produced by ^{3}He bombardment of ^{16}O; these are ^{13}O (threshold, 37.38 MeV) and ^{9}C (threshold, 47.16 MeV). At 45-MeV bombarding energy, production of ^{13}O may be anticipated, but with a half-life of ~9 msec[33,34] it should not be observed in the representative spectra shown in Figs. 2 and 3. This conclusion is confirmed by comparing these spectra with that[34] of ^{13}O; no common peaks are

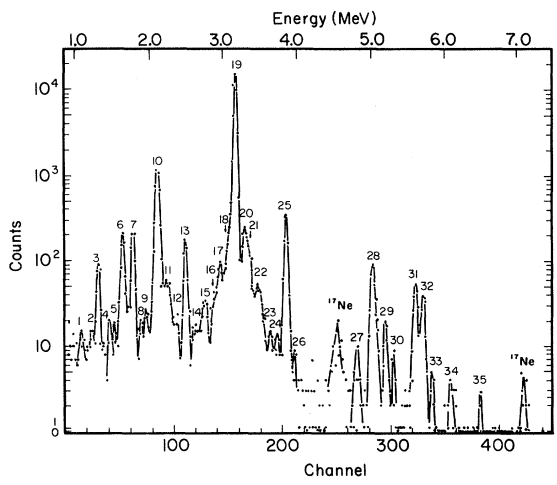

FIG. 4. Spectrum of delayed protons observed in a counter telescope with a 14-μ ΔE counter following 35-MeV ^{3}He bombardment of CS_2. The proton laboratory energy is indicated at the top. All numbered peaks except No. 11 are identified with the decay of ^{33}Ar; they correspond to the data in Table II.

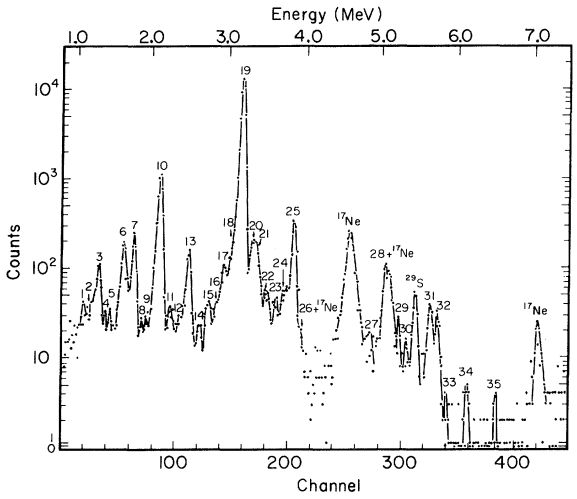

FIG. 5. Spectrum of delayed protons observed under the same conditions as for Fig. 4 except that a 55-MeV ^{3}He beam was used for bombardment.

observed. Further, delayed-proton percursors cannot be produced at this bombarding energy from titanium (in the TiO_2 targets). The principal peaks in the spectra have previously been identified as following the decay of ^{17}Ne by threshold and cross-bombardment measurements.[10,11] That all peaks were due to ^{17}Ne decay was further corroborated by the eight time-sorted energy spectra; within their statistical accuracy all peaks exhibit the same lifetime.

A number of delayed-proton precursors can be produced by ^{3}He bombardment of sulphur. At 35 MeV (see Fig. 4), however, only ^{33}Ar and ^{29}S (thresholds[1] 19.50 and 29.00 MeV, respectively) can be produced, together with ^{13}O (from carbon present in the CS_2 target). Protons from the decay of ^{13}O can be eliminated as they were in the ^{17}Ne discussion, and no peaks from the known spectrum[35] of ^{29}S could be discerned. The possibility of delayed-proton precursors arising from reactions on light contaminants in the target was investigated by comparing the spectrum in Fig. 4 with known delayed-proton spectra.[10,36] Only ^{17}Ne, produced from an oxygen contaminant, was observed, but its strongest peak was a factor of 10^3 smaller than that of ^{33}Ar. Again, the principal peaks in Fig. 4 have previously been identified[13,14] as originating with the decay of ^{33}Ar, and all have the same lifetime within statistics.

At 55-MeV bombarding energy (see Fig. 5) the peaks from ^{17}Ne are stronger and a ^{29}S peak at ~5.4 MeV has appeared, but no additional peaks are observed. All numbered peaks have the same relative intensities (after subtracting known ^{17}Ne strength) except peak 11 which is much weaker. Its origin could not be established but it clearly *cannot* be ^{33}Ar.

B. Energy Measurements

Energy calibration was initially derived from the spectrum in Fig. 5. Peak 19 and the peak labeled ^{29}S have previously been assigned[13,14,35] to protons emitted from the $T = \frac{3}{2}$ analog states in ^{33}Cl and ^{29}P, respectively. These states have also been observed in proton-resonance studies[37,38] on ^{32}S

TABLE I. Observed proton peaks following ^{17}Ne decay, and deduced energies in ^{17}F. All observed energies are quoted in the c.m. system as (MeV ± keV) and are preceded by underlined numbers relating them to peaks in the spectra of Figs. 2 and 3. Those spaces marked X correspond to proton groups predicted from the deduced energy levels to be within our range of observation, but which were not in fact seen. Those marked ··· represent groups predicted to be outside our range of observation (≲1 MeV).

Observed proton energies, corresponding to decay to the following ^{16}O states: g.s.	6.052 MeV	6.131 MeV	6.916 MeV	7.115 MeV	Deduced level energies in ^{17}F (MeV ± keV)
4 2.484 ± 30					3.084 ± 30
8 4.009 ± 15					4.609 ± 15
10 4.880 ± 10					5.480 ± 10
11 5.437 ± 10					6.037 ± 10
12 5.806 ± 30					6.406 ± 30
13 7.108 ± 30	X	···	···		7.708 ± 30
14 7.474 ± 10	1 1.434 ± 25	X	···	···	8.075 ± 10
15 7.837 ± 10	2 1.771 ± 30	X	···	···	8.436 ± 10
16 8.232 ± 30	3 2.163 ± 35	X	X	X	8.825 ± 25
17 10.597 ± 4 [a]	X	9 4.458 ± 10	7 3.658 ± 30	6 3.481 ± 20	11.197 ± 4 [a]
Unassigned proton peak [b]: 5 2.825 ± 30					

[a] The energy of this level was taken from Ref. 1, and the proton peak corresponding to its ground-state decay was used in part to establish the calibration.

[b] The possible origin of this peak in discussed in the text.

and ^{28}Si, and from those results the energies of our proton peaks can be calculated to have lab energies of 3.170 ± 0.004 MeV and 5.437 ± 0.005 MeV, respectively. Using pulser calibration points to establish the linearity of the scale and these two points to determine the absolute values, energies were determined for all peaks in Fig. 5. In particular, the energy of the ^{17}Ne peak at ~4.6 MeV was accurately determined and the result applied to the analysis of Fig. 2, where it is labeled peak 10. Peak 17 in the spectrum of Fig. 2 corresponds to decay of the lowest $T = \frac{3}{2}$ analog state in ^{17}F, and its energy is accurately known.[1] Again, these two points permit energy measurements to be made for all peaks in the spectrum and, by extrapolation, for those in Fig. 3 as well. Energies determined from these and seven other independently recorded spectra of ^{17}Ne decay are listed in Table I, where the underlined numerals appearing before the energies correspond to the peak labels in Figs. 2 and 3. The energies for delayed-proton peaks in the ^{33}Ar decay were obtained from Figs. 4 and 5, and are listed in Table II.[39,40]

C. Half-Life Measurements

By requiring that recorded events satisfy stringent ΔE coincidence requirements and identify as protons, very little background due to electrons is evident in the spectra. In addition, only protons from a single activity (with the exceptions already noted) appear in a given spectrum. Thus, measured lifetimes should not suffer from possible systematic errors caused by an unrecognized additional activity as might those measured by other techniques. Nevertheless, the two methods described in Sec. III were both used in a number of separate runs; no significant difference was ever found between the eight-point decay curves (for

TABLE II. Observed proton peaks following ^{33}Ar decay, and deduced level energies in ^{33}Cl. All observed energies are quoted in the c.m. system as (MeV ± keV) and are preceded by underlined numbers relating them to peaks in the spectra of Figs. 4 and 5. Those spaces marked X correspond to proton groups predicted from the deduced energy levels to be within our range of observation, but which were not in fact seen. Those marked ··· represent groups predicted to be outside our range of observation (i.e., ≲1.0 MeV).

Observed proton energies corresponding to decay to the following ^{32}S states: g.s.	2.237 MeV	3.780 MeV	Deduced level energies [a] in ^{33}Cl (MeV ± keV)
6 1.692 ± 20			3.973 ± 20
7 1.837 ± 20			4.118 ± 20
10 2.174 ± 20			4.455 ± 20
12 2.439 ± 35	···		4.720 ± 35
13 2.566 ± 15	···		4.847 ± 16
15 2.835 ± 25	···		5.116 ± 25
18 3.165 ± 30	···		5.446 ± 30
19 3.269 ± 4[d]	···		5.550 ± 6 [b]
20 3.403 ± 20	1 1.126 ± 35		5.675 ± 17
21 3.469 ± 30	2 1.264 ± 35		5.763 ± 23
22 3.592 ± 35[c]	3 1.364 ± 30		5.882 ± 31
23 3.751 ± 35	4 1.519 ± 35		6.034 ± 25
24 3.859 ± 35	5 1.587 ± 40	···	6.125 ± 26
25 3.973 ± 20	X	···	6.254 ± 20
27 4.984 ± 40	14 2.687 ± 30	X	7.228 ± 25
28 5.189 ± 20	16 2.975 ± 40	X	7.475 ± 18
29 5.342 ± 30	17 3.048 ± 30	X	7.595 ± 22
30 5.486 ± 40	X	X	7.767 ± 40
31 5.803 ± 20	22 3.592 ± 35[c]	9 2.022 ± 30	8.084 ± 17
32 5.902 ± 25	22 3.592 ± 35[c]	X	8.183 ± 25
33 6.029 ± 30	X	X	8.310 ± 30
34 6.310 ± 40	26 4.106 ± 35	X	8.609 ± 27
35 6.688 ± 30	X	X	8.969 ± 30

Unassigned proton peaks[d]: 8 1.947 ± 30, 11 2.303 ± 35

[a] The level energies were calculated using −21.005 ± 0.004 MeV as the mass excess of ^{33}Cl; it is a weighted average of the results in Refs. 18, 39, and 40.

[b] The energy of the lowest $T = \frac{3}{2}$ state was taken from Ref. 37 and corrected for the ^{33}Cl mass excess.

[c] The weak proton peak at $E_{cm} = 3.592$ MeV is broad and could involve several groups; it therefore appears more than once in the table.

[d] The possible origin of these peaks is disucssed in the text.

TABLE III. Half-lives of ^{9}C, ^{17}Ne, and ^{33}Ar.

Parent	Weighted average of present measurements (msec)	Previous results (msec)	Ref.
^{17}Ne	109.0±1.0	105±5	11
		103±7	10
		107±5	41
^{33}Ar	173.0±2.0	182±5	15
		178±10	12,13
^{9}C	126.5±1.0	127±3	27
		126.5±2	28

which a particular peak was integrated at successive times), and the 400-point curves multiscaled from a chosen peak or peaks in the proton spectrum. In no case was a second lifetime component required to fit the data.

The averaged results from a series of runs are shown in Table III,[41] where they are compared with previous results. As a final check for any systematic errors the lifetime of ^{9}C was measured, and this result also appears in the table. Agreement with the previous results[27,28] for ^{9}C is excellent.

D. ^{17}Ne Decay

In deciding the energy level responsible for a given proton peak, a certain ambiguity arises: Does it feed the ground state or an excited state of the final nucleus, in this case ^{16}O? Usually the measured energies, when compared with known levels in the nuclei involved, are sufficient to resolve the difficulty. However, in the case of ^{17}Ne decay a difficulty arises because the first two excited states in ^{16}O are separated by only 80 keV. To clarify this point, p-γ coincidences were measured, as discussed in Sec. III. All observed protons must be associated with 511-keV γ rays from annihilation of the positrons which feed levels in ^{17}F. Since the 6.052-MeV state in ^{16}O is 0^+, it decays by internal pair conversion, and protons leading to this state will be characterized by twice the expected rate of coincidences with annihilation radiation. In the bottom portion of Fig. 3 is a spectrum of those protons coincident with 511-keV γ rays; it was obtained simultaneously with the singles spectrum also appearing in that figure. Note that the relative heights of peaks 1, 2, and 3 are approximately doubled in the coincidence spectrum. This is expressed quantitatively in Table IV where the coincidence rates for these three peaks are compared with that for peak 10, the strongest in the spectrum. Their coincidence rate is greater and indicates that they most probably correspond to proton decays leading to the 0^+ first excited state of ^{16}O.

The measured energies listed in Table I confirm this result, since they too are consistent with peaks 1, 2, and 3 feeding the 6.052-MeV state in ^{16}O. This table lists the energies of levels in ^{17}F which account for the observed proton spectrum, and these deduced energy levels are compared with previously obtained level energies in Table V.[42-46] An interesting result of this comparison is that our results resolve the discrepancy between Salisbury and Richards[42] and Harris, Philips, and Jones[43] concerning the energy of the $\frac{3}{2}^-$ states at 4.6 and 5.5 MeV.[47] The effects of momentum broadening mentioned in Sec. III make difficult the extraction of precise level widths from our data, but a comparison between the widths listed in Table V and the proton spectra in Figs. 2 and 3 shows good qualitative agreement. In fact, the assignment of peaks 6, 7, and 9 to the decay of the $T=\frac{3}{2}$ analog state[47] can be based not only on their measured energies but also on their observed narrow width.

Many channels are energetically allowed for decay of the analog state. These are listed in Table VI[48-50] together with our experimental values or upper limits for intensities where they fall within our range of observation. Calculated penetration factors[50] are also shown for each decay channel; it is evident that proton decay to the 1^- state at 9.614 MeV in ^{16}O is the only unobserved channel for which significant decay might occur.

Relative intensities were measured for all peaks in the spectra of Figs. 2 and 3. The results were then used to determine relative intensities for the

TABLE IV. Results of proton-γ (511 keV) coincidence measurements for ^{17}Ne decay.

Proton energy (MeV)	Proton-singles counts	Proton-γ (511 keV) coincidence counts [a]	Coincidences / singles (%)
$\underline{1}$ 1.434	289±20	12.1±5.3	4.2±1.9
$\underline{2}$ 1.771	638±28	39.7±7.1	6.2±1.1
$\underline{3}$ 2.163	177±15	7.3±3.3	4.1±1.9
$\underline{10}$ 4.880	8889±95	266.4±16.8	2.5±0.2

[a] These numbers have been corrected for the chance- and background-coincidence counting rate.

preceding β^+-decay branches using the assignments made in Table I, and these intensities are listed in the second column of Table VII. The errors quoted on the branch to the $T=\frac{3}{2}$ state at 11.97 MeV include the errors and limits listed in Table VI; the unobserved proton branch from this state to the 1^- level in ^{16}O at 9.614 MeV was assigned an intensity limit of <0.05 based on its calculated penetrability and the observed intensity to the 1^- state at 7.115 MeV. Energetically allowed but experimentally unobservable decays for $T=\frac{1}{2}$ states are indicated in Table I; their calculated penetrabilities are all significantly less than those for observed decays. Consequently, ignoring them will have little effect on the results. At worst, an additional unobserved proton channel will affect the intensity of the corresponding β transition but will not alter the intensities of other transitions beyond their stated uncertainties. Finally, the observed branching and reduced-width ratios for the four $T=\frac{1}{2}$ states above 7 MeV are shown in Table VIII.

E. ^{33}Ar Decay

To establish the origin of observed proton groups, particle-γ coincidences were again recorded for the decay of ^{33}Ar. No part of the proton spectrum appeared to be associated with 2.2-MeV γ rays from the deexcitation of the first excited state in ^{32}S, and it was thus concluded that all of the stronger peaks (numbers 6, 7, 10, 13, 18, 19, 20, 21, and 25 in Figs. 4 and 5) must correspond to proton decay to the ground state of ^{32}S. Based on the energies of observed proton peaks, levels in ^{33}Cl which must be fed in the β^+ decay of ^{33}Ar were deduced and listed in Table II. Our energies are compared with previously known levels in Table IX, where the agreement obtained is excellent.

Observed intensities and the assignments in Table II were used to determine relative β^+-branch intensities, and these are listed in the second column of Table X. The observed proton-branching and reduced-width ratios for states above 5.6 MeV in ^{33}Cl are shown in Table XI. The decay of the lowest $T=\frac{3}{2}$ state in ^{33}Cl to the first excited state in ^{32}S is energetically allowed but of too low an energy to be detected by our system. However, the penetration factor calculated[50] for such a decay channel is smaller by a factor of $\sim 10^4$ than it is for decay to the ground state. Consequently, only the ground-state proton decay of the analog state was considered in determining the β^+-branch intensi-

TABLE V. Comparison of observed energy levels in ^{17}F with previous results.

Present results (MeV ± keV)	Previous work Ref. 42[a] (MeV ± keV)[c]	Ref. 43[a] (MeV ± keV)[c]	Ref. 44[b] (MeV ± keV)[c]	Other (MeV ± keV)	Γ[a, b] (MeV)	J^π
3.084 ± 30		3.10 ± 20		3.106 ± 7[d]	0.020	$\frac{1}{2}^-$
4.609 ± 15	4.698 ± 10	4.60 ± 20			0.240	$\frac{3}{2}^-$
5.480 ± 10	5.526 ± 10	5.47 ± 20			0.073	$\frac{3}{2}^-$
6.037 ± 10	6.046 ± 10				0.030	$\frac{1}{2}^-$
6.406 ± 30				6.43 ± 80[e]		$(\frac{1}{2},\frac{3}{2})^-$
7.708 ± 30			7.75 ± 10[f]		0.190	$(\frac{1}{2},\frac{3}{2})^-$
8.075 ± 10			8.09 ± 10[f]		0.110	$(\frac{1}{2},\frac{3}{2})^-$
8.436 ± 10			8.45 ± 10[f]		0.045	$(\frac{1}{2},\frac{3}{2})^-$
8.825 ± 25						$(\frac{1}{2},\frac{3}{2})^-$
				11.197 ± 4[g]	0.0005[h]	$\frac{1}{2}^-, T=\frac{3}{2}$

[a] ^{16}O$(p,p)^{16}$O.

[b] ^{16}O$(p,p)^{16}$O, ^{16}O$(p,p')^{16}$O, ^{16}O$(p,\alpha)^{13}$N.

[c] The uncertainty quoted with these results includes only the uncertainty in the incident proton energy. The discrepancy between Refs. 42 and 43 indicates that the errors in determining some resonance energies is considerably larger.

[d] ^{16}O$(p,p)^{16}$O; see Ref. 45.

[e] Delayed proton emission; see Ref. 11.

[f] The spins and parities assigned these states in Ref. 44 are not consistent with their being fed by allowed β^+ decay from ^{17}Ne. Nevertheless, the agreement in energies and in observed decay channels makes it appear plausible that we are observing the same state. The possibility of unresolved doublets cannot, of course, be ruled out.

[g] See Ref. 1.

[h] See Ref. 46.

TABLE VI. Energetically allowed particle decays of the 11.197-MeV, $T=\frac{3}{2}$ state in ^{17}F.

	Final state [a] (MeV)	J^π	Energy of decay particle [b] (MeV)	Penetration factor P [c]	Observed intensity I [d] (%)	I/P [e]	Particle branching ratio [f] (%)
$p+^{16}$O	0.000	0^+	10.597	2.3	0.074±0.016	0.032	10±2 [g]
	6.052	0^+	4.545	1.0	<0.02	<0.02	
	6.131	3^-	4.466	0.4	0.160±0.015	0.40	22±2 [g]
	6.916	2^+	3.681	0.8	0.174±0.040	0.22	24±6
	7.115	1^-	3.482	1.1	0.313±0.025	0.28	44±4
	8.870	2^-	1.727	0.02	h		
	9.614	1^-	0.983	0.10	•••		
	9.847	2^+	0.750	0.009	•••		
	10.353	4^+	0.244	$<10^{-8}$	•••		
$\alpha+^{13}$N	0.00	$\frac{1}{2}^-$	5.379	2.3	<0.05	<0.022	
	2.366	$\frac{1}{2}^+$	3.013	0.4	<0.05	<0.125	
	3.509	$\frac{3}{2}^-$	1.870	0.008	•••		
	3.547	$\frac{5}{2}^+$	1.832	0.001	•••		

[a] The energy levels of ^{16}O are taken from Browne and Michael (see Ref. 48); those in ^{13}N come from the review of Ajzenberg-Selove (see Ref. 49).

[b] These energies are expressed in the c.m. system.

[c] $P=kR/(F_L^2+G_L^2)$ evaluated at a radius of 1.25 $(A_1^{1/3}+A_2^{1/3})$ fm, where F_L and G_L are the regular and irregular Coulomb functions, respectively, taken from Ref. 50, and L is the lowest allowed angular momentum transfer.

[d] These intensities are expressed as percentages of the total proton decay of ^{17}Ne. Spaces marked ••• correspond to predicted energies outside our range of observation.

[e] I/P is the % intensity (column 6) divided by the penetration factor (column 5).

[f] This branching refers only to the particle decay of the 11.197-MeV state in ^{17}F.

[g] These numbers agree well with results from the ^{15}N(^{3}He,n)^{17}F(11.20)(p)^{16}O reaction [A. B. MacDonald, E. G. Adelberger, H. B. Mak, D. Ashery, A. P. Shukla, C. L. Cocke, and C. N. Davids, Phys. Letters 31B, 119 (1970)], where the branching ratio to the ^{16}O ground state is determined to be (9±2)% and to the unresolved 6.05- and 6.13-MeV states, (23±5)%.

[h] No limit could be set on the intensity of this branch, since it coincided with another proton group.

TABLE VII. β^+ branching ratios and ft values for ^{17}Ne β^+ ^{17}F.

Energy level in ^{17}F (MeV)	Proportion of proton emissions (%)	Branching ratio from ^{17}Ne (%)	ft [a] (sec)	logft (sec)
0.000	•••	0.53±0.16 [b]	$(8.85\pm2.70)\times10^6$	6.95±0.13
0.500	•••	1.1±0.5 [b]	$(3.56\pm1.60)\times10^6$	6.55±0.21
3.105 [c]	0.49±0.07	0.48±0.07	$(2.78\pm0.41)\times10^6$	6.44±0.06
4.609	16.5±0.7	16.2±0.7	$(3.91\pm0.18)\times10^4$	4.59±0.02
5.480	54.9±0.5	54.0±0.7	$(7.19\pm0.16)\times10^3$	3.86±0.01
6.037	10.8±0.2	10.6±0.2	$(2.61\pm0.07)\times10^4$	4.42±0.01
6.406	0.36±0.10	0.35±0.10	$(6.24\pm1.82)\times10^5$	5.80±0.13
7.708	0.18±0.05	0.18±0.05	$(4.70\pm1.30)\times10^5$	5.67±0.12
8.075	6.94±0.1	6.83±0.11	$(9.19\pm0.29)\times10^3$	3.96±0.01
8.436	6.61±0.26	6.51±0.26	$(7.02\pm0.34)\times10^3$	3.85±0.02
8.825	1.93±0.06	1.90±0.06	$(1.68\pm0.08)\times10^4$	4.23±0.02
11.197	$0.72^{+0.10}_{-0.05}$	$0.71^{+0.10}_{-0.05}$	$(1.93^{+0.17}_{-0.29})\times10^3$	$3.29^{+0.04}_{-0.07}$
$E_p=2.825$ [d]	0.55±0.05	0.54±0.05		

[a] The ft values are calculated using 16.517±0.026 MeV as the mass excess (Ref. 1) of ^{17}Ne and 109.0±1.0 msec as its half-life.

[b] These ratios are calculated by comparison with the mirror ^{17}N decay.

[c] This energy is the average of our present result with those listed in Table V.

[d] The c.m. energy of this proton group is listed since the level from which it originates is uncertain.

TABLE VIII. Particle branching ratios from $T=\frac{1}{2}$ states in ^{17}F.

^{17}F state (MeV)	Observed relative branching ratio ^{16}O(6.05)/^{16}O(0.00)	$\gamma^2(6.05)/\gamma^2(0.00)$ [a]
7.708	<5.0	<240
8.075	0.49±0.02	7.9
8.436	6.0±0.5	57
8.825	8.2±1.2	52

[a] γ^2 is the reduced width. This ratio is obtained from column 2 by dividing the branching ratios by their respective penetration factors.

ties shown in Table X.

Since allowed β^+-decay branches of ^{33}Ar were expected to feed one excited state of ^{33}Cl below the proton separation energy, γ spectra were recorded using the Ge(Li) counter. A typical spectrum is shown in Fig. 6. Since four time-sorted spectra were recorded in the same manner as for proton spectra, the identification of peaks was aided by lifetime measurements; energy calibration was obtained by using a ^{56}Co source before and after each run. The origin of each significant peak is marked in the figure and, in more detail, in Table XII. One γ ray, at 810 keV, is positively identified from its measured half-life and energy as following the decay of ^{33}Ar. It corresponds to deexcitation of the first excited state[18,40] of ^{33}Cl. No γ rays from the decay of other low-lying states in ^{33}Cl were observed (i.e., they total <7% of the 810-keV γ-ray intensitity). Since γ-ray and proton spectra were recorded simultaneously, relative γ-ray-to-proton intensity values were obtained by using the known efficiency of each detector (see Sec. III) and dead times determined by continuously recording a pulser in each system. The result indicated that the γ-ray intensity was 1.42±0.24 times that of all delayed protons.

V. ANALYSIS AND DISCUSSION

A. ^{17}Ne Decay

In order to convert the relative proton intensities listed in Table VII into absolute *ft* values, it is necessary to determine the intensities of the first-forbidden β^+-decay branches to the ground and first excited states of ^{17}F. This is done by comparison with the mirror decay of ^{17}N using the techniques described in Sec. II C. The relative proton intensities are then renormalized to give the β^+ branching ratios listed in the third column of Table VII. The *ft* values and their logarithms are then calculated directly and appear in the last two columns of the table. We have calculated the statistical rate function, f [see Eqs. (1) and (11)] taking into account the finite nuclear size ($R=1.3\times A^{1/3}$ fm)

TABLE IX. Comparison of observed levels below 6 MeV in ^{33}Cl with previous results. Only those levels below 6 MeV are shown, since none above that energy have been reported previously with comparable error bars; our complete results appear in Table II.

Present results (MeV±keV)	Previous work [a] Ref. 18 (MeV±keV)	Ref. 40 [b] (MeV±keV)	Other (MeV±keV)	Γ [c] (MeV)	Average level energy (MeV)	J^π
3.973±20	3.984±4	3.982±4		0.0015	3.983±3	$\frac{3}{2}^+$
4.118±20	4.123±4	4.123±4	4.119±10 [d]	0.0085	4.123±3	$\frac{3}{2}^+$
4.455±20	4.444	4.441±4		<0.002	4.442±4	$\frac{3}{2}^+$
4.720±35	4.746	4.751±4		<0.002	4.751±4	$\frac{5}{2}^-$
4.847±16	4.831	4.837±4		<0.002	4.838±4	$\frac{3}{2}^+$
5.116±25	5.110±4	5.111±4		0.0015	5.111±4	$\frac{3}{2}^+$
5.446±30	5.455±6			0.032	5.455±6	$\frac{1}{2}^+$
			5.550±6 [e]	0.0015 [e]	5.550±6	$\frac{1}{2}^+$, $T=\frac{3}{2}$
5.675±17	5.656±10 [f]			0.100	5.675±17	$(\frac{1}{2}^+, \frac{3}{2}^+)$
5.763±23	5.743±6			0.040	5.744±6	$\frac{1}{2}^+$
5.882±31	5.884±4 [f]			0.001	5.882±31	$(\frac{1}{2}^+, \frac{3}{2}^+)$

[a] All previous results have been corrected, where necessary, to take account of the ^{33}Cl mass excess being −21.005±0.004 MeV.

[b] ^{32}S$(p,\gamma)^{33}$Cl.

[c] Taken from Refs. 18 and 40.

[d] ^{32}S$(^3$He$,d)^{33}$Cl; see Ref. 39.

[e] ^{32}S$(p,p)^{32}$S; see Ref. 37.

[f] The spins and parities assigned these states in Ref. 18 are not consistent with their being fed by allowed β^+ decay from ^{33}Ar. Nevertheless, the agreement in energies and in observed decay channels makes it appear plausible that we are seeing the same states. Since the possibility of unresolved doublets cannot be ruled out, the two energies were not averaged.

TABLE X. β^+ branching ratios and ft values for $^{33}\mathrm{Ar} \xrightarrow{\beta^+} {}^{33}\mathrm{Cl}$.

Energy level [a] in ^{33}Cl (MeV)	Proportion of proton emissions (%)	Branching ratio from ^{33}Ar (%)	ft [b] (sec)	logft (sec)
0.000	•••	18.1 ± 1.9 [c]	$(1.06 \pm 0.11) \times 10^5$	5.03 ± 0.05
0.810	•••	48.1 ± 3.6	$(2.74 \pm 0.21) \times 10^4$	4.44 ± 0.03
3.983	1.19 ± 0.05	0.40 ± 0.04	$(5.14 \pm 0.55) \times 10^5$	5.71 ± 0.05
4.123	1.26 ± 0.05	0.43 ± 0.05	$(4.32 \pm 0.53) \times 10^5$	5.64 ± 0.05
4.442	7.41 ± 0.13	2.50 ± 0.26	$(5.75 \pm 0.64) \times 10^4$	4.76 ± 0.05
4.751	0.14 ± 0.02	0.047 ± 0.008	$(2.45 \pm 0.43) \times 10^6$	6.39 ± 0.08
4.838	0.92 ± 0.05	0.31 ± 0.04	$(3.46 \pm 0.43) \times 10^5$	5.54 ± 0.05
5.111	0.24 ± 0.03	0.081 ± 0.013	$(1.06 \pm 0.17) \times 10^6$	6.03 ± 0.07
5.455	1.68 ± 0.06	0.57 ± 0.06	$(1.11 \pm 0.13) \times 10^5$	5.05 ± 0.05
5.550	78.9 ± 0.8	26.7 ± 2.7	$(2.18 \pm 0.24) \times 10^3$	3.34 ± 0.05
5.675	1.63 ± 0.06	0.55 ± 0.06	$(9.4 \pm 1.1) \times 10^4$	4.97 ± 0.05
5.744	1.09 ± 0.04	0.37 ± 0.04	$(1.31 \pm 0.16) \times 10^5$	5.12 ± 0.05
5.882	$0.68^{+0.38}_{-0.19}$	$0.23^{+0.13}_{-0.07}$	$(1.84^{+1.04}_{-0.57}) \times 10^5$	5.26 ± 0.18
6.034	0.08 ± 0.02	0.027 ± 0.007	$(1.35 \pm 0.36) \times 10^6$	6.13 ± 0.12
6.125	0.05 ± 0.02	0.017 ± 0.007	$(1.96 \pm 0.92) \times 10^6$	6.29 ± 0.22
6.254	1.73 ± 0.06	0.58 ± 0.06	$(5.01 \pm 0.60) \times 10^4$	4.70 ± 0.05
7.228	0.12 ± 0.02	0.041 ± 0.008	$(2.23 \pm 0.47) \times 10^5$	5.35 ± 0.09
7.475	0.86 ± 0.04	0.29 ± 0.03	$(2.24 \pm 0.29) \times 10^4$	4.35 ± 0.06
7.595	0.74 ± 0.04	0.25 ± 0.03	$(2.17 \pm 0.31) \times 10^4$	4.34 ± 0.06
7.767	0.03 ± 0.01	0.010 ± 0.003	$(4.2 \pm 1.3) \times 10^5$	5.62 ± 0.14
8.084	$0.67^{+0.38}_{-0.19}$	$0.23^{+0.13}_{-0.07}$	$(1.07^{+0.67}_{-0.37}) \times 10^4$	4.05 ± 0.20
8.183	$0.41^{+0.38}_{-0.19}$	$0.14^{+0.13}_{-0.07}$	$(1.47^{+1.37}_{-0.75}) \times 10^4$	4.17 ± 0.30
8.310	0.05 ± 0.01	0.017 ± 0.004	$(9.5 \pm 2.2) \times 10^4$	4.98 ± 0.10
8.609	0.05 ± 0.01	0.017 ± 0.004	$(5.2 \pm 1.4) \times 10^4$	4.71 ± 0.12
8.969	0.01 ± 0.005	0.003 ± 0.0015	$(1.22 \pm 0.64) \times 10^5$	5.09 ± 0.25
$E_p = 1.947$ [d]	0.07 ± 0.02	0.024 ± 0.007		

[a] The values below 6 MeV are averages taken from Table IX. Above that energy they are from the present work only.
[b] The ft values are calculated using (−9.400 ± 0.050) MeV as the mass excess of ^{33}Ar and 173.0 ± 2.0 msec as its half-life. The mass was calculated using the isobaric-mass formula and the results in Refs. 1 and 37.
[c] This ratio is calculated by comparison with the mirror ^{33}P decay.
[d] The c.m. energy of this proton group is listed, since the level from which it originates is uncertain.

TABLE XI. Particle branching ratios from states in ^{33}Cl.

^{33}Cl (MeV)	Observed relative branching ratios ^{32}S(2.24)/^{32}S(0.00)	$\gamma^2(2.24)/\gamma^2(0.00)$ [a] $\frac{1}{2}^+$	$\frac{3}{2}^+$	Observed relative branching ratios ^{32}S(3.78)/^{32}S(0.00)	$\gamma^2(3.78)/\gamma^2(0.00)$ [a] $\frac{1}{2}^+$	$\frac{3}{2}^+$
5.675	0.027 ± 0.011	84	0.41			
5.744	0.052 ± 0.017	83	0.50			
5.882	>0.87	>960	>6.9			
6.034	2.7 ± 1.7	1400	12.4			
6.125	2.8 ± 2.7	1180	11.8			
6.254	<0.028	<8.3	<0.09			
7.228	2.1 ± 0.8	67	2.5			
7.475	0.26 ± 0.04	5.9	0.27			
7.595	5.7 ± 0.8	121	5.6			
7.767	Ref. b	•••	•••			
8.084	<1.6	<19	<1.4	0.36 ± 0.06	4.1	28
8.183	<2.5	<36	<2.2			
8.310	<0.15	<1.3	<0.13			
8.609	0.48 ± 0.28	3.6	0.36			
8.969	<2.0	<13	<1.5			

[a] γ^2 is the reduced width. This ratio is obtained from the observed value by dividing each branching ratio by its respective penetration factor (see Ref. 50), assuming either $\frac{1}{2}^+$ or $\frac{3}{2}^+$ as the J^π for the state in ^{33}Cl. The interaction radius was taken to be 5.2 fm.
[b] No limit could be set on the intensity of this branch, since it coincided with another proton group.

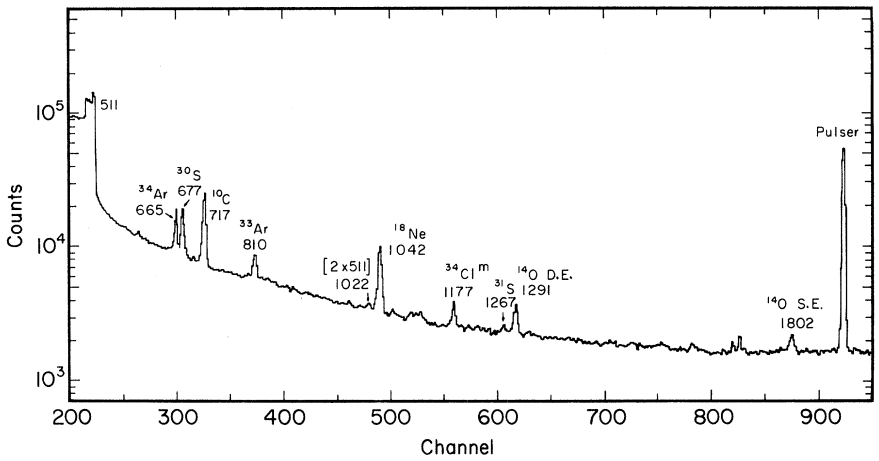

FIG. 6. Spectrum of γ rays observed following 35-MeV ^{3}He bombardment of CS_2. The parent and the decay energy in keV is marked for each significant peak; a more detailed description is given in Table XII.

and the effects of screening by the atomic electrons.[51] The quoted errors include uncertainties in the measured intensities, lifetimes, and decay energies, where the mass taken for ^{17}Ne was that calculated with the isobaric multiplet mass equation,[1] since there are no experimental measurements of comparable accuracy. A decay scheme for ^{17}Ne encompassing the present results is shown in Fig. 7.

Log*ft* values less than 6.0 are characteristic of allowed decay, which in the case of ^{17}Ne indicates $\frac{1}{2}^-$ or $\frac{3}{2}^-$ for the final-state spin and parity. These assignments appear in Table V and again in the figure; where unique values are given, they arise from previous work (e.g., Ref. 42). It should be pointed out that the proton peak at 2.825 MeV could not be positively assigned to the decay of any particular level; if it were assumed to feed the ground state of ^{16}O a new state in ^{17}F must be proposed at low excitation energy, and if it were assumed to feed an excited state it is not clear which one, or why the corresponding ground-state decay is unobserved. Nevertheless, there is no reason to doubt that it is associated with the decay of ^{17}Ne, and it was included in determining the intensities quoted in Table VII.

Detailed calculations for levels in ^{17}F, which include up to two particles in the $(2s, 1d)$ shell and

TABLE XII. γ rays observed following bombardment of CS_2 with 35-MeV ^{3}He particles.

Observed γ rays (keV)	Transition responsible	Previously measured γ energy (keV)	Previously measured β^+ half-life (sec)
665 ± 2	^{34}Ar$(\beta^+)^{34}$Cl$^{***}(\gamma)^{34}$Cl	664.6 ± 0.3 [a]	b
677 ± 2	^{30}S$(\beta^+)^{30}$P$^*(\gamma)^{30}$P	677.8 ± 0.9 [c]	1.4 [c]
717.3 ± 0.8 [d]	^{10}C$(\beta^+)^{10}$B$^*(\gamma)^{10}$B	717.3 ± 0.8 [e]	19.4 [e]
810 ± 2	^{33}Ar$(\beta^+)^{33}$Cl$^*(\gamma)^{33}$Cl	810 ± 3 [f]	0.173 [g]
1042 ± 2	^{18}Ne$(\beta^+)^{18}$F$^{**}(\gamma)^{18}$F	1041.7 ± 0.6 [h]	1.67 [i]
1177 ± 2	^{34}Cl$^m(\beta^+)^{34}$S$^{**}(\gamma)^{34}$S*	1177.0 ± 1.2 [c]	1.57 [c]
1267 ± 3	^{31}S$(\beta^+)^{31}$P$^*(\gamma)^{31}$P	1266.1 ± 0.2 [c]	2.61 [c]
1290.79 ± 0.06 [d]	^{14}O$(\beta^+)^{14}$N$^*(\gamma$ D.E.$)^{14}$N	1290.79 ± 0.06 [j]	71.0 [j]
1801.80 ± 0.06 [d]	^{14}O$(\beta^+)^{14}$N$^*(\gamma$ S.E.$)^{14}$N	1801.80 ± 0.06 [j]	71.0 [j]

[a] H. D. Graber and G. J. Harris, Phys. Rev. 188, 1685 (1969).
[b] Values quoted in Ref. 18 are 1.2 ± 0.3 sec and 0.85 ± 0.10 sec. Our results indicate a half-life of 0.91 ± 0.05 sec.
[c] See Ref. 18.
[d] Used as calibration.
[e] T. Lauritsen and F. Ajzenberg-Selove, Nucl. Phys. 78, 1 (1966).
[f] Average of results quoted in Refs. 18 and 40.
[g] Obtained from the present delayed-proton results.
[h] E. K. Warburton, J. W. Olness, and A. R. Poletti, Phys. Rev. 155, 1164 (1967).
[i] D. E. Alburger and D. H. Wilkinson, Phys. Letters 32B, 190 (1970).
[j] F. Ajzenberg-Selove, California Institute of Technology Report No. LAP-82 (unpublished).

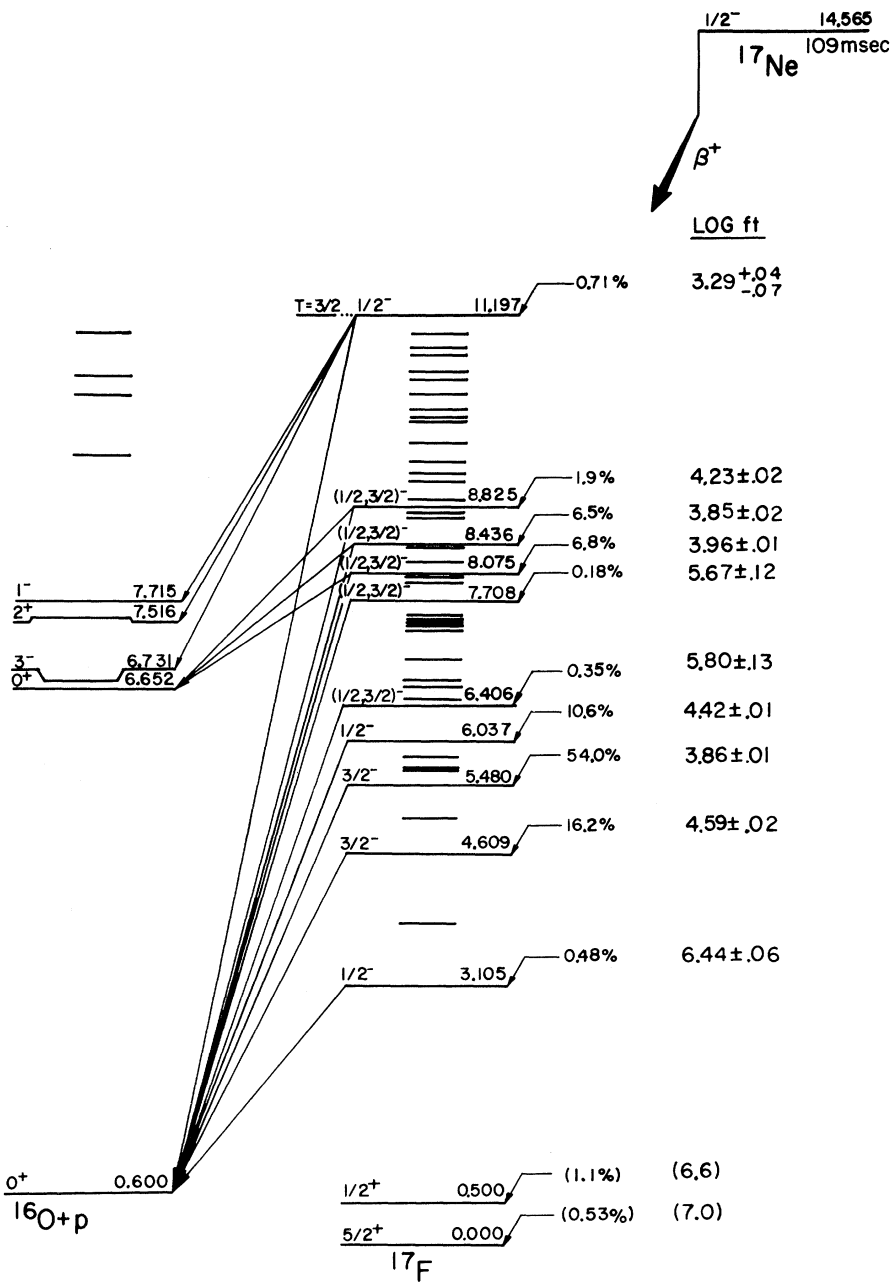

FIG. 7. Proposed decay scheme of ^{17}Ne. The ^{17}F level energies above 4 MeV are the values determined from the present experiment (except the 11.197-MeV state).

one hole in the $1p$ shell, have been reported by Margolis and de Takacsy.[52] There is reasonable qualitative agreement between our observed β^+ transitions and their calculations: Of the ten $\frac{1}{2}^-$ and $\frac{3}{2}^-$ levels predicted below 10 MeV, we observe nine, and we could not have seen levels above 8 MeV fed by decays with logft values $\gtrsim 5.5$. In the calculations, the wave function for the $(T=\frac{3}{2})$ ground state of ^{17}Ne and its analog in ^{17}F is well represented by a $(1p_{1/2})$ hole coupled to the lowest 0^+ $(T=1)$ state in mass 18 (e.g., the ground state of ^{18}Ne). The same components coupled to $T=\frac{1}{2}$ have a form generally referred to as the antianalog configuration, the major component of which is expected to be contained in the $\frac{1}{2}^-$ state at 3.105 MeV in ^{17}F. Though the β^+ decay to this level is very weak, this can be explained as being due to cancellations caused by details of the wave function.[53] In fact, these cancellations can be used to deduce from our measured ft value that between 80 and

85% of the antianalog configuration is contained therein. The remainder of its strength is predicted to lie at about 6 [52] or 8 MeV [53] in a state which is fed by a transition with a very low logft value (~3.4). We observe three states at about 8 MeV with logft values ≤ 4.23, it appears likely that one or several of these contain the missing component. Since isospin mixing is expected to be relatively large between the analog state and its corresponding antianalog configuration, it is particularly interesting that some of the latter's strength lies so near in energy.

Finally, we can compare the mirror decays of ^{17}Ne and ^{17}N. The method used is to calculate transition strengths in ^{17}N assuming strict mirror symmetry with the observed decays in ^{17}Ne. A half-life for ^{17}N is thus calculated and compared with the measured value of 4.16 ± 0.04 sec,[54] yielding [see Eq. (10)] $\delta = 0.15 \pm 0.03$. This is not in particularly good agreement with the value $\delta = 0.065$ calculated[55] from the apparent systematics[19,21] discussed in Sec. II B. However, before the significance of this disagreement can be assessed, it will be necessary to remeasure the ^{17}N lifetime and, preferably, to determine precisely the intensities of its individual β^--decay branches.

B. ^{33}Ar Decay

The ground-state β^+-decay branch from ^{33}Ar was calculated by the technique described in Sec. II B and, together with the relative γ-to-proton intensity measurement, was used to renormalize the proton intensities in Table X. The β^+ branching ratios and ft values for ^{33}Ar decay are also listed in the table, and many appear in the decay scheme shown as Fig. 8; they were calculated in the same way as those for ^{17}Ne.

In this case not all branches necessarily correspond to allowed decay, since several with logft > 6.0 have been observed. In particular, the state at 4.751 MeV has previously been assigned $J = \frac{5}{2}$, and the intensity we observe for β decay feeding the state requires negative parity (indicating first-forbidden decay) rather than positive (second forbidden). Assigned J^π values for states below 6 MeV are shown in Table IX where unique values result from previous measurements. All states we observe above 6 MeV can be assigned as $(\frac{1}{2}, \frac{3}{2})^+$ except those at 6.034 and 6.125 MeV, which may not be fed by allowed β decay.

For the same reasons as those discussed for ^{17}Ne decay, a single proton peak (at 1.947 MeV) could not be assigned to the decay of any particular level. It was included, however, in the intensities in Table X.

The calculations of Glaudemans, Wiechers, and

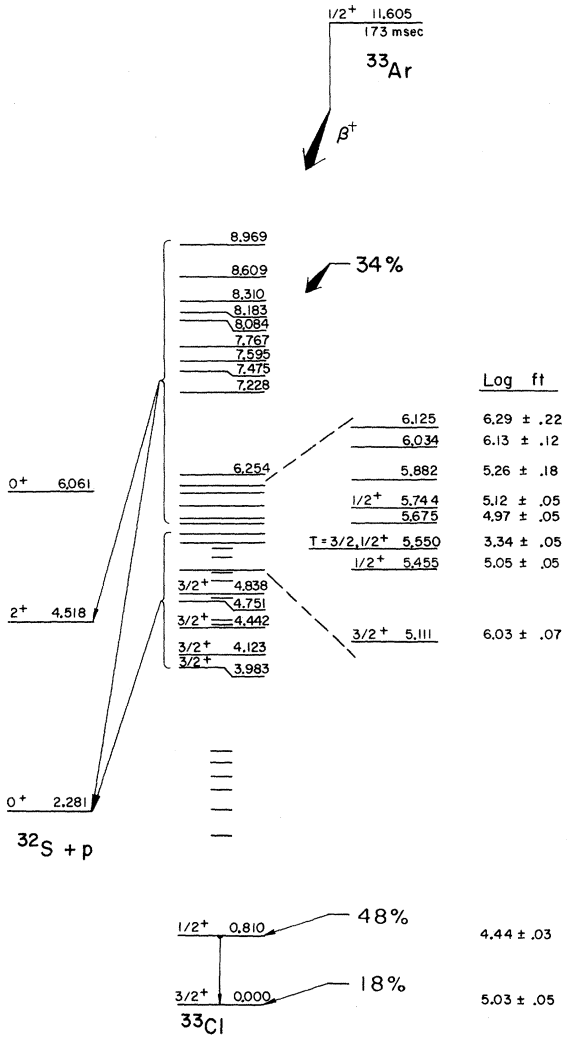

FIG. 8. Proposed decay scheme of ^{33}Ar. The ^{33}Cl level energies below 6 MeV are average values determined from the present and earlier experiments (see Table IV). Above that energy the values are from the present work only.

Brussaard[56] for the levels in ^{33}Cl consider only particles in the $2s_{1/2}$ and $1d_{3/2}$ shells. Below 9 MeV, 16 levels are predicted to be $\frac{1}{2}^+$ or $\frac{3}{2}^+$, compared with 22 allowed β-decay transitions observed in this experiment. This disagreement undoubtedly reflects the contributions present from other orbitals, and any more detailed quantitative comparison would not be justified.

C. Isospin Purity

The ft values measured for the superallowed decay branches from ^{17}Ne and ^{33}Ar are shown in Table XIII where they are compared with values calculated assuming (i) model calculations[17] and (ii) the limiting case, $\langle\sigma\rangle^2 = 0$; these calculations have

TABLE XIII. Isospin purity of lowest $T=\frac{3}{2}$ states in ^{17}F and ^{33}Cl.

Nucleus	Superallowed ft value feeding analog state: Experimental (sec)	Superallowed ft value feeding analog state: Calculated [a] (sec)	Limit (i.e., $\langle\sigma\rangle^2=0$) (sec)	Isospin purity ($=100\,a^2$) (%)
^{17}F	$(1.93^{+0.17}_{-0.29})\times10^3$	1.96×10^3	$\leq 2.06\times10^3$	>95
^{33}Cl	$(2.18\pm0.24)\times10^3$	1.82×10^3	$\leq 2.06\times10^3$	81 ± 9 [95^{+5}_{-10}] [b]

[a] See Ref. 17.

[b] The bracketed value applies if $\langle\sigma\rangle^2=0$.

been discussed in Sec. II A. The isospin purity a^2, expressed as a percent, is also shown.

Evidently for ^{17}Ne there is no indication of significant isospin mixing. For ^{33}Ar, on the other hand, the situation is not so clear. If the model calculations are to be believed, quite considerable mixing is indicated, and even in the limiting case $\langle\sigma\rangle^2=0$, a possible impurity remains. Further evidence of isospin mixing between the $T=\frac{3}{2}$ state and surrounding $T=\frac{1}{2}$ states is provided by the measured logft values for the latter states; these values become progressively lower the nearer in energy the states are to the analog level. This effect is displayed in the expanded section of Fig. 8. It is possible to calculate an upper limit on the magnitude of the $T=\frac{3}{2}$ component admixed into these $T=\frac{1}{2}$ states by assuming that the strength of the β^+ decay feeding them is derived entirely from their $T=\frac{3}{2}$ impurity. (In essence, we are taking the limit, $\langle\sigma\rangle^2=0$.) For the four levels nearest the analog state (i.e., those at 5.455, 5.675, 5.744, and 5.882 MeV) this corresponds to between 1 and 2% $T=\frac{3}{2}$ strength in each level. Certainly this is of the right order to account for the strength missing from the analog state itself. It is now possible to calculate the charge-dependent matrix elements using Eq. (6); for the four levels in question these range in magnitude from 13 to 35 keV. A survey of measured matrix elements for 0^+ states has been published by Bloom,[57] and it shows that the majority of the 26 known examples lie between 1 and 40 keV. Thus the mixing we have suggested – even though it is an upper limit – is well within the limits suggested by these other measurements. However, because of the proximity of the interacting levels, the actual wave-function impurities in our case are possibly much larger than for those surveyed.[57]

Although the measurement of a high logft value for the superallowed decay is incontrovertible evidence for isospin impurity in the analog state, the observed low logft values for surrounding decays are only circumstantial evidence that the mixing has occurred with the nearby $T=\frac{1}{2}$ states. It is certainly possible that the Gamow-Teller matrix elements alone could account for the decay strength, and that they exhibit the observed clustering because of the presence of a configuration at that excitation energy which is simply related to the parent-state wave function.[58] In addition, mixing only occurs between states of the same spin and parity, and of the four nearby $T=\frac{1}{2}$ states only two are known to be $\frac{1}{2}^+$; we can only restrict the others to $(\frac{1}{2},\frac{3}{2})^+$. On the other hand, if 5 to 10% of the $T=\frac{3}{2}$ strength is missing from the analog state, the expected size of the charge-dependent matrix element[57] restricts the source of the mixing to nearby states. For example 5% mixing with the $\frac{1}{2}^+$ state at 810 keV in ^{33}Cl would imply a matrix element of ~1 MeV, which is an order of magnitude higher than any known example.

D. Configurations of $T=\frac{1}{2}$ Admixtures

Proton decay from a pure $T=\frac{3}{2}$ state in ^{17}F or ^{33}Cl is forbidden, since it cannot conserve isospin (assuming the final state is purely $T=0$). Thus by examining the proton-decay channels it may be possible to deduce the nature of the $T=\frac{1}{2}$ admixture through which the decay proceeds. For a case such as the lowest analog state in ^{33}Cl, decay only to the ground state of ^{32}S is indicated on the basis of calculated penetrabilities (see Sec. IV E) and no information about the wave function can be extracted. But for ^{17}Ne, a number of states in ^{16}O are energetically available and certain simple conclusions regarding the admixed configuration can be made. The antianalog configuration alluded to in Sec. V A has the form $|(sd)^2(p_{1/2})^3;\ \frac{1}{2}^-,\ \frac{1}{2}\rangle$, where the notation indicates two particles in the $(2s,1d)$ shell and three particles (one hole) in the $(1p_{1/2})$ shell coupled to a total J^π, T of $\frac{1}{2}^-$, $\frac{1}{2}$. If this were the chief source of $T=\frac{1}{2}$ strength in the analog state, then one would expect to observe proton decay to levels in ^{16}O which involve the configurations $|(sd)^2(p_{1/2})^2;J,0\rangle$ or $|(sd)(p_{1/2})^3;J,0\rangle$. The calculations of Zuker, Buck, and McGrory[59] for states in ^{16}O indicate that the ground state and the lowest excited states with 3^-, 2^+, and 1^- do indeed have strong components of this type and that the first excited 0^+ state does not. This is in agreement with our observations (see Table VI) and

lends credence to the postulate that the antilog configuration is responsible for $T = \frac{1}{2}$ mixing.

These ideas can be extended quantitatively by taking the total strength for these configurations in the ground and first four excited states of ^{16}O; the approximate values in ascending order of excitation energy are 34, 0, 66, 29, and 48%. These are in good agreement with the trend of the reduced widths for corresponding transitions as reflected by the numbers in the second to last column of Table VI. Certainly the approximate nature of this calculation, where the details of *sd*-shell configurations have been neglected, precludes a firm conclusion. However, there is strong indication that the antianalog configuration plays the dominant role. This agrees very well with the calculations of Walker and Schlobohm,[60] who take a very simple form for the analog-state wave function but reach the same conclusion. They also predict a very small (<1%) total impurity in the analog state in agreement with our results.

IV. ACKNOWLEDGMENTS

We should like to thank J. A. Macdonald for his assistance during the data acquisition, and D. A. Landis for designing and building the valve-control electronics. One of us (J.C.H.) would like to thank the Miller Institute for Basic Research in Science for a fellowship held during the course of part of this work.

---

†Work performed under the auspices of the U. S. Atomic Energy Commission.

*Present address: Chalk River Nuclear Laboratories, Chalk River, Ontario, Canada.

[1]J. Cerny, Ann. Rev. Nucl. Sci. 18, 27 (1968).

[2]J. Jänecke, Nucl. Phys. A128, 632 (1969).

[3]J. C. Hardy, J. M. Loiseaux, J. Cerny, and G. T. Garvey, to be published.

[4]M. Tomaselli, Z. Physik 233, 240 (1970).

[5]G. F. Trentelman, B. M. Preedom, and E. Kashy, Phys. Rev. Letters 25, 530 (1970); R. Mendelson, G. J. Wozniak, A. D. Bacher, J. M. Loiseaux, and J. Cerny, Phys. Rev. Letters 25, 533 (1970).

[6]W. H. MacDonald, in *Nuclear Spectroscopy*, edited by F. Ajzenberg-Selove (Academic Press Inc., New York, 1960), p. 932.

[7]R. Barton, R. McPherson, R. E. Bell, W. R. Frisken, W. T. Link, and R. B. Moore, Can. J. Phys. 41, 2007 (1963).

[8]G. N. Flerov, V. A. Karnaukhov, G. M. Ter-Akopyan, L. A. Petrov, and V. G. Subbotin, Nucl. Phys. 60, 129 (1964).

[9]Activity with a ~690-msec half-life was attributed to ^{17}Ne by J. M. d' Auria and I. L. Preiss, Phys. Letters 10, 300 (1964); subsequent work (see Refs. 10 and 11, and the present report) indicates that ^{17}Ne, with a half-life of ~110 msec, could not be responsible.

[10]R. McPherson, J. C. Hardy, and R. E. Bell, Phys. Letters 11, 65 (1964); J. C. Hardy and R. E. Bell, Can. J. Phys. 43, 1671 (1965).

[11]R. A. Esterlund, R. McPherson, A. M. Poskanzer, and P. L. Reeder, Phys. Rev. 156, 1094 (1967).

[12]J. C. Hardy and R. I. Verrall, Phys. Rev. Letters 13, 764 (1964).

[13]J. C. Hardy and R. I. Verrall, Can. J. Phys. 43, 418 (1965).

[14]P. L. Reeder, A. M. Poskanzer, and R. A. Esterlund, Phys. Rev. Letters 13, 767 (1964).

[15]A. M. Poskanzer, R. McPherson, R. A. Esterlund, and P. L. Reeder, Phys. Rev. 152, 995 (1966).

[16]E. J. Konopinski and M. E. Rose, in *Alpha-, Beta-, and Gamma-Ray Spectroscopy*, edited by K. Siegbahn (North-Holland Publishing Company, Amsterdam, The Netherlands, 1965), p. 1327; R. J. Blin-Stoyle, in *Isospin in Nuclear Physics*, edited by D. H. Wilkinson (North-Holland Publishing Company, Amsterdam, The Netherlands, 1969), p. 115.

[17]J. C. Hardy and B. Margolis, Phys. Letters 15, 276 (1965).

[18]P. M. Endt and C. van der Leun, Nucl. Phys. A105, 1 (1967).

[19]D. H. Wilkinson, Phys. Letters 31B, 447 (1970).

[20]J. N. Huffaker and E. Greuling, Phys. Rev. 132, 738 (1963).

[21]D. H. Wilkinson and D. E. Alburger, Phys. Rev. Letters 24, 1134 (1970) ($A = 20, 25$); D. E. Alburger and D. H. Wilkinson, Phys. Letters 32B, 190 (1970) ($A = 18$).

[22]M. G. Silbert and J. C. Hopkins, Phys. Rev. 134, B16 (1964).

[23]H. J. Schopper, *Weak Interactions and Nuclear Beta Decay* (North-Holland Publishing Company, Amsterdam, The Netherlands, 1966).

[24]J. P. Davidson, Jr., Phys. Rev. 82, 48 (1951).

[25]J. E. Esterl, R. G. Sextro, J. C. Hardy, G. J. Ehrhardt, and J. Cerny, to be published.

[26]F. S. Goulding, D. A. Landis, J. Cerny, and R. H. Pehl, Nucl. Instr. Methods 31, 1 (1964).

[27]J. C. Hardy, R. I. Verrall, R. Barton, and R. E. Bell, Phys. Rev. Letters 14, 376 (1965).

[28]J. M. Mosher, R. W. Kavanagh, and T. A. Tombrello, Bull. Am. Phys. Soc. 14, 1167 (1969).

[29]We should like to thank David Allred for fabricating these targets.

[30]H. L. Scott and D. M. Van Patter, Phys. Rev. 184, 1111 (1969).

[31]Obtained from the International Atomic Energy Agency, Vienna, Austria.

[32]C. M. Lederer, J. M. Hollander, and I. Perlman, *Table of Isotopes* (John Wiley & Sons, Inc., New York, 1967).

[33]R. McPherson, R. A. Esterlund, A. M. Poskanzer, and P. L. Reeder, Phys. Rev. 140, B1513 (1965).

[34]J. E. Esterl, J. C. Hardy, R. G. Sextro, and J. Cerny, Phys. Letters 33B, 287 (1970).

[35]J. C. Hardy and R. I. Verrall, Phys. Letters 13, 148 (1964).

[36]For ^{25}Si: P. L. Reeder, A. M. Poskanzer, R. A. Esterlund, and R. McPherson, Phys. Rev. 147, 781

(1966); ^{32}Cl: J. E. Steigerwalt, J. W. Sunier, and J. R. Richardson, Nucl. Phys. A137, 585 (1969); ^{37}Ca and ^{41}Ti: see Ref. 15; ^{40}Sc: R. I. Verrall and R. E. Bell, Nucl. Phys. A127, 635 (1969).

[37]R. Van Bree, H. Ogata, and G. M. Temmer, Bull. Am. Phys. Soc. 13, 1402 (1968).

[38]D. H. Youngblood, G. C. Morrison, and R. E. Segel, Phys. Letters 22, 625 (1966); B. Teitelman and G. M. Temmer, Phys. Letters 26B, 371 (1968).

[39]C. E. Moss, Nucl. Phys. A145, 423 (1970).

[40]J. W. Gordon, Ph. D. thesis, University of Kansas, Lawrence, Kansas (unpublished).

[41]T. H. Braid, A. M. Friedman, and R. W. Fink, Bull. Am. Phys. Soc. 10, 120, 168 (1965).

[42]S. R. Salisbury and H. T. Richards, Phys. Rev. 126, 2147 (1962). The energies reported by these authors must be corrected to take account of errors found in the calibration of the analysis magnet used to determine the incident proton energies (J. C. Davis, private communication). For all energies quoted in the present work, this correction has been applied.

[43]R. W. Harris, G. C. Philips, and C. M. Jones, Nucl. Phys. 38, 259 (1962).

[44]R. L. Dangle, L. D. Oppliger, and G. Hardie, Phys. Rev. 133B, 647 (1964). The energies quoted from this work have been corrected for a calibration error; see note with Ref. 42.

[45]V. Gomes, R. A. Douglas, T. Polga, and O. Sala, Nucl. Phys. 68, 417 (1965).

[46]J. R. Patterson, H. Winkler, and C. S. Zaidins, Phys. Rev. 163, 1051 (1967).

[47]The level energies of Salisbury and Richards (see Ref. 42) were used to provide an internal energy calibration for our delayed-proton spectrum in a preliminary report of this work [J. C. Hardy, J. E. Esterl, R. G. Sextro, and J. Cerny, in *Nuclear Isospin*, edited by J. O. Anderson, S. D. Bloom, J. Cerny, and W. W. True (Academic Press Inc., New York, 1969), p. 725]. The effect of their incorrect energy assignment on our work was the misassignment of one decay branch of the analog state to the 0^+ level at 6.052 MeV in ^{16}O. Our present results show that the branch in question leads to the 3^- state at 6.131 MeV (see Table I).

[48]C. P. Browne and I. Michael, Phys. Rev. 134B, 133 (1964).

[49]F. Ajzenberg-Selove, Nucl. Phys. A152, 1 (1970).

[50]W. T. Sharp, H. E. Gove, and E. B. Paul, Atomic Energy of Canada Limited, Report No. AECL-268 (unpublished).

[51]J. N. Bahcall, Nucl. Phys. 75, 10 (1966).

[52]B. Margolis and N. deTakacsy, Can. J. Phys. 44, 1431 (1966).

[53]B. Margolis and N. deTakacsy, Phys. Letters 15, 329 (1965).

[54]Average of results quoted in F. Ajzenberg-Selove and T. Lauritsen, Nucl. Phys. 11, 1 (1959), and S. Hinds, R. Middleton, A. E. Litherland, and D. J. Pullen, Phys. Rev. Letters 6, 113 (1961).

[55]The energy $W_0^+ + W_0^- = 12.5$ MeV was determined by averaging over the individual transitions weighted by their branching ratios.

[56]P. W. M. Glaudemans, G. Wiechers, and P. J. Brussaard, Nucl. Phys. 56, 548 (1964).

[57]S. D. Bloom, in *Isobaric Spin in Nuclear Physics*, edited by J. D. Fox and D. Robson (Academic Press Inc., New York, 1966), p. 123.

[58]V. A. Karnaukhov, Yadern Fiz. 10, 450 (1969) [transl.: Soviet J. Nucl. Phys. 10, 257 (1970)].

[59]A. P. Zuker, B. Buck, and J. B. McGrory, Phys. Rev. Letters 21, 39 (1968).

[60]G. E. Walker and D. Schlobohm, Nucl. Phys. A140, 49 (1970); G. E. Walker, private communication.

PHYSICAL REVIEW C VOLUME 3, NUMBER 2 FEBRUARY 1971

Coulomb Excitation of the First 2^+ State of ^{24}Mg†

D. Vitoux,* R. C. Haight,‡ and J. X. Saladin

Department of Physics, University of Pittsburgh, Pittsburgh, Pennsylvania 15213

(Received 28 September 1970)

Coulomb excitation of the first excited state of ^{24}Mg has been investigated by means of a coincidence experiment using a position-sensitive detector. Interpreting the data according to the semiclassical theory and correcting for quantal effects, we obtained a reduced transition probability of $B(E2; 0^+ \rightarrow 2^+) = 0.042 \pm 0.002\ e^2 b^2$ and a static quadrupole moment of $Q_{2+} = -0.305 \pm 0.064\ e$ b.

I. INTRODUCTION

In recent years, higher-order effects in Coulomb excitation (including the so-called reorientation effect) have been used extensively to determine spectroscopic quadrupole moments of excited nuclear states.[1] A large number of experiments have been performed on medium-heavy and heavy nuclei. It was of interest to extend those measurements to light nuclei, in particular to ^{24}Mg, whose excitation spectrum displays quasirotational features. In this region, the standard experimental techniques used in heavier nuclei present some technical difficulties, however, and various new methods have been developed. Bamberger, Bizetti, and Povh[2] have measured the quadrupole moment of the first excited state of ^{24}Mg by looking at the line shape of the 1.37-MeV γ rays emitted at 0°.